COPY NO.
RM No. E8F04

NACA

RESEARCH MEMORANDUM

DESIGN AND PERFORMANCE OF EXPERIMENTAL AXIAL-DISCHARGE MIXED-FLOW COMPRESSOR

I - IMPELLER DESIGN THEORY

By Arthur W. Goldstein

Flight Propulsion Research Laboratory
Cleveland, Ohio

TECHNICAL EDITING WAIVED

NATIONAL ADVISORY COMMITTEE FOR AERONAUTICS

WASHINGTON
August 12, 1948

NACA RM No. E8F04 RESTRICTED

NATIONAL ADVISORY COMMITTEE FOR AERONAUTICS

RESEARCH MEMORANDUM

DESIGN AND PERFORMANCE OF EXPERIMENTAL AXIAL-DISCHARGE MIXED-FLOW COMPRESSOR

I - IMPELLER DESIGN THEORY

By Arthur W. Goldstein

SUMMARY

An axial-discharge mixed-flow compressor, which is especially adapted for jet engines because of the large mass flow per unit frontal area, is described. The basic concept of the design procedure is the incorporation of conditions for efficient flow into the design equations so that all reasonable cases can be computed without investigating the effect of a large number of design parameters. General equations of relative fluid motion are developed to show clearly the assumptions involved, and the empirical character of the simplifications employed to render the system of equations solvable and to complete the design.

The best impeller was selected on the basis of the maximum air-flow capacity, which was 19.6 pounds per second for a 14-inch-diameter impeller with a tip speed of 1480 feet per second and a pressure ratio of 3.5.

INTRODUCTION

The centrifugal compressor has the advantage of high pressure ratio in a single stage, simple construction, mechanical strength, compactness, and reliability, but is handicapped by relatively low efficiency and low mass flow per unit frontal area. For high-speed jet engines, the frontal area is important from the standpoint of drag and mass flow is important from the standpoint of power. The axial-flow compressor, on the other hand, has the advantage of high efficiency, high air-flow capacity per unit frontal area, and ease of staging, but is complicated and expensive to manufacture, fragile, and relatively heavy. A compressor combining the best features of these two types would be rendered compact, simple, light, and strong by accomplishing the compression in rotors of high blade

solidity and work output, and would be reduced to a small frontal area by having the air directed axially at the entrance and exit of the impeller and in the diffuser. The apparent lower efficiency of the centrifugal compressor could probably be improved by the development of a more rational method of design, thus justifying the development of a compressor with high blade solidity and compression in a single stage.

A compressor of this type was therefore developed with a maximum internal diameter of 14 inches including the diffuser, an equivalent tip speed of 1480 feet per second based on stagnation inlet conditions, and a compression ratio of 3.5. The air flow was to be maximized in the design process.

AERODYNAMIC BASIS OF DESIGN

The basic problem of the design is to assign the correct velocity distribution at the impeller entrance and exit and to select dimensions that will produce maximum weight flow for a prescribed outer diameter, rotative speed, and pressure ratio. A study of the effect of all design variables on air-flow capacity, however, is a stupendous task because of the large number of cases that must be computed. Relations between the design parameters are therefore established on the basis of certain assumptions as to how the air could be efficiently handled and the independent variables are reduced to two, thus permitting an evaluation of all reasonable designs with minimum effort.

Equations of flow at the entrance and exit are first developed and these flows are related by means of conditions for efficiently handling the air. This part of the design is completed with a maximized flow before the impeller shape is determined. An impeller shape is then computed to accomplish the desired change in air flow and state from the entrance to the exit. General equations of motion in the impeller are developed in order to indicate clearly the basic assumptions made in obtaining the shape of the impeller hub. Appropriate simplifications are used to permit an easy solution for the impeller design. Stream-filament methods are used in determining the velocity distribution and blade shape in the inducer section, and from this point downstream a faired curve is used for the blade camber line.

Basic Assumptions

The following assumptions are used in establishing flow relations and velocity distribution:

1. At the entrance and exit (stations 1 and 3 in fig. 1), the entropy is constant on an axial plane, which is the equivalent of assuming no boundary layer on the shrouds and equal entropy increases for all streamlines in the impeller.

2. The gas inside the impeller flows on surfaces of revolution.

3. Tangential velocity at the casing in the discharge annulus is 0.95 of the tip speed.

4. The velocity reduction at the blade tips in the inducer section is one-third the incoming relative velocity.

5. Pressure rise allowed on the case is slightly less than the centrifugal pressure rise on the assumption that the boundary layer limits the pressure rise.

6. At the exit, the maximum allowed absolute Mach number is 1.4.

7. At the entrance, the maximum allowed relative Mach number is 1.0.

For computing the shape of the impeller there are the following assumptions:

1. The blade tips are shaped according to two-dimensional stream-filament theory, which is applied to compute the velocity on the blade surface. Suitability of the velocity distribution is judged by two-dimensional boundary-layer theory. The rest of the blade, extending down to the root, is shaped to maintain radial blade elements.

2. Inside the impeller the entropy is constant on surfaces of revolution normal to the meridional projection of the streamlines.

3. The frictional forces on only the blades and impeller are taken into account; those on the case are neglected.

4. An infinite number of blades is assumed for computing the hub shape.

Determination of Entrance and Exit Conditions

At the entrance, it is assumed that radial equilibrium exists at the impeller face. For balance of the centrifugal and pressure forces

$$\frac{1}{\rho}\frac{dp}{dr} = \frac{V_u^2}{r} \tag{1}$$

where

p pressure

r radius

V absolute gas velocity

ρ density

Subscript:

u rotational component

From thermodynamics, with the assumption of constant entropy,

$$dH = \frac{1}{\rho}\,dp \tag{2}$$

and

$$H = H_t - \frac{V^2}{2} \tag{3}$$

where

H enthalpy

Subscript:

t stagnation state

Substitution gives

$$\frac{dH}{dr} = \frac{dH_t}{dr} - \frac{d}{dr}\left(\frac{V^2}{2}\right) = \frac{V_u^2}{r} \tag{4}$$

At the entrance, the stagnation enthalpy is constant because of the constant energy level, and (4) reduces to

$$\frac{d}{dr}\left(\frac{V_a^2}{2}\right) = -\frac{1}{2r^2}\frac{d}{dr}(rV_u)^2 \tag{5}$$

where the subscript a indicates the axial velocity component. The mass flow W between the cylinder of radius r and the case r_c is

$$W = 2\pi \int_r^{r_c} \rho V_a r dr \tag{6}$$

The impellers considered are to have subsonic internal relative flow and the relative velocity at the entrance blade tips is therefore assumed to be sonic. The mathematical expression for this condition is

$$(V_{a,c,1})^2 = \frac{2}{\gamma+1}\left[(a_{t,1})^2 + 2\omega(r_{c,1}V_{u,c,1}) - \omega^2 (r_{c,1})^2\right] - (V_{u,c,1}r_{c,1})^2/(r_{c,1})^2 \tag{7}$$

where

a sonic velocity

γ ratio of specific heats

ω angular velocity

Subscripts:

c case

1 impeller entrance

Station numbers and some dimensions and flow parameters are shown in figure 1. For convenience, the symbols used in the text and appendix A are listed in appendix B.

With these three equations for the entrance flow, insufficient relations are available to establish the flow there. At the exit, additional conditions are required to prevent the work output and exit Mach number from varying too much. In order to apply equations (5), (6), and (7) it is therefore necessary to relate the entrance to the exit flow and to apply the conditions imposed on the exit flow to determine the entrance flow.

Flow on Impeller Blade Tips

The gas near the blade tips is assumed to be compressed to such a degree in the inducer section that the boundary layer on the blade tips will separate from the blades with a further pressure rise in a reasonable distance. Downstream of the end of the inducer, a pressure rise in the radial direction slightly less than that due to centrifugal force is therefore allowed at the case. In symbolic notation,

$$dp < \rho\omega^2 r_c \, dr_c$$

There is an entropy rise of the air and the pressure rise is therefore arbitrarily reduced

$$\frac{1}{\rho}\frac{dp}{dr_c} = \omega^2 r_c - T\frac{dS}{dr_c}$$

where

S entropy

T absolute temperature

But

$$\frac{1}{\rho}\frac{dp}{dr_c} = -T\frac{dS}{dr_c} + \frac{dH}{dr_c}$$

and Euler's equation combined with the energy equation gives for any streamline

$$dH_t = \omega d(rV_u) = d\left(H + \frac{V^2}{2}\right)$$

Therefore,

$$\omega^2 r_c = \frac{\omega d(r_c V_{u,c})}{dr_c} - \frac{d}{dr_c}\left(\frac{V_c^2}{2}\right)$$

If the relative velocity v is introduced, the solution of the equations is found to be

$$v_c = \text{constant} = v_{c,2} = v_{c,3} \tag{8}$$

where the subscript 2 indicates the end of the inducer section before radial flow begins and 3 indicates conditions at the impeller exit. A compression in the inducer is estimated as feasible with

$$v_{c,2} = \frac{2}{3} v_{c,1} = \frac{2}{3}\left[(V_{a,c,1})^2 + (V_{u,c,1} - \omega r_{c,1})^2\right]^{1/2} \tag{9}$$

Flow at Impeller Exit

If the blade tips at the exit are directed axially at this point the tangential component of the velocity is

$$V_{u,c,3} = v_{u,c,3} + \omega r_{c,3} = f\,\omega r_{c,3} \tag{10}$$

where f is the slip factor. For the impellers under consideration, eighteen blades are used, and an estimate gives $f = 0.95$. The axial-flow component is then

$$V_{a,c,3} = v_{a,c,3} = \sqrt{(v_{c,3})^2 - (v_{u,c,3})^2} = \sqrt{(v_{c,2})^2 - (1-f)^2\,\omega^2\,(r_{c,3})^2} \tag{11}$$

In the discharge annulus the velocity components will vary in some manner from the values at the tip. If a linear variation of the quantity $(V_{u,3})^2/r_3$ is prescribed,

$$\frac{(V_{u,3})^2}{r_3} = \frac{(V_{u,h,3})^2}{r_{h,3}} + \frac{\left[(V_{u,c,3})^2/r_{c,3}\right] - \left[(V_{u,h,3})^2/r_{h,3}\right]}{(r_{c,3} - r_{h,3})}(r_3 - r_{h,3}) \tag{12}$$

where subscript h indicates the inner-radius (hub) or blade-root value. The enthalpy at the exit is a fundamental compressor performance parameter, and is, of course, related to the exit velocities. Because of limits to be imposed on the exit gas velocity at the blade roots, the enthalpy at the exit will be related to the Mach numbers of the absolute and relative flow at the blade roots in the discharge annulus. If equation (4) is now applied at the exit and (12) is substituted, the resultant equation can be integrated to give

$$H_3 - H_{h,3} = \left[\frac{V^2_{u,h,3}}{r_{h,3}} + \left(\frac{V^2_{u,c,3}}{r_{c,3}} - \frac{V^2_{u,h,3}}{r_{h,3}}\right) \frac{(r_3 - r_{h,3})}{2(r_{c,3} - r_{h,3})}\right] \left[r_3 - r_{h,3}\right] \tag{13}$$

or

$$H_{c,3} - H_{h,3} = \left[\frac{r_{c,3} - r_{h,3}}{2}\right] \left[\frac{(V_{u,h,3})^2}{r_{h,3}} + \frac{(V_{u,c,3})^2}{r_{c,3}}\right] \tag{14}$$

The Mach number at the exit must not be too high for efficient diffusion. Its value is given by

$$M_3^2 = \frac{V_3^2}{(\gamma-1)H_3} = \frac{V_3^2}{(\gamma-1)H_{t,3}} \Bigg/ \left(1 - \frac{V_3^2}{2H_{t,3}}\right) \tag{15}$$

The relative Mach number M' is also of significance because its magnitude will indicate choking flow in the impeller. It is related to other flow variables by

$$(M'_3)^2 = \frac{(v_3)^2}{(\gamma-1)H_3} = \frac{(V_{a,3})^2 + (V_{u,3} - \omega r_3)^2}{(\gamma-1)\ H_3}$$

$$(M'_3)^2 = (M_3)^2 + \frac{\omega^2(r_3)^2 - 2\omega r_3 V_{u,3}}{(\gamma-1)\ H_3} \tag{16}$$

The value of H_3 at the root $(H_{h,3})$ from (16) is substituted in (14) to give the value at the case related to the Mach numbers at the root

$$H_{c,3} = \frac{2\omega r_{h,3} V_{u,h,3} - \omega^2 (r_{h,3})^2}{(\gamma-1)\left[(M_{h,3})^2 - (M'_{h,3})^2\right]} + \frac{(r_{c,3} - r_{h,3})}{2}\left(\frac{(V_{u,h,3})^2}{r_{h,3}} + \frac{(V_{u,c,3})^2}{r_{c,3}}\right) \qquad (17)$$

There are now available sufficient relations to determine the complete flow at the entrance and exit with only two independent parameters, provided there are reasonable limitations on the flow conditions. A number of designs are therefore computed with various assigned values of these parameters and the design is selected on the basis of the best air-flow capacity. The assumptions and procedures for computing the entrance and exit velocities are now summarized.

SCHEDULE OF DESIGN COMPUTATIONS

For all impellers to be designed, the work output per pound is assigned and known. Consequently, from the state of the entering gas $(p_{t,1}, H_{t,1})$, $H_{t,c,3}$ is known. The work output varies from streamline to streamline, and therefore the mean work output per pound is known only approximately. The rotative velocity ω and the maximum frontal dimension $r_{c,3}$ are also assigned.

Computations at Case

1. From the assigned data, $v_{u,c,3}$ and $V_{u,c,3}$ are computed by means of (10), which assumed axially directed blades at the exit near the case. The Euler equation

$$H_{t,3} - H_{t,1} = \omega(r_3 V_{u,3} - r_1 V_{u,1}) \qquad (18)$$

can then be used to find the entering moment of momentum at the case $(r_{c,1}V_{u,c,1})$.

2. The particular design being investigated now enters into consideration by assigning values to $r_{c,1}$ and $r_{h,3}$. The assigned value of $r_{c,1}$ permits the computation of $V_{u,c,1}$ from $(r_{c,1}V_{u,c,1})$. The value of $r_{h,3}$ is only tentative because in some cases the entrance annulus will not accommodate the entire exit flow. Therefore, when the minimum permissible $r_{h,1}$ is computed, the corresponding streamline position at the exit must be found and the exit annulus cut off at that position.

3. Equation (7) is used to find $V_{a,c,1}$. A relative Mach number of 1.0 at the entrance blade tips is assumed.

4. For the exit at the case, equations (8) and (9) give $v_{c,1}$, $v_{c,2}$, and $v_{c,3}$. With $v_{c,3}$ and $v_{u,c,3}$ equation (11) determines $V_{a,c,3}$ which with $V_{u,c,3}$ is used to find $V_{c,3}$. Then the enthalpy $H_{c,3}$ is computed from

$$H = H_t - \frac{V^2}{2} \tag{19}$$

By assuming an efficiency for the impeller (0.85), it is possible to find $p_{t,c,3}$ and $\rho_{c,3}$ from

$$\rho_{c,3} = \left(\frac{H_{c,3}}{H_{t,c,3}}\right)^{\frac{1}{\gamma-1}} \frac{p_{t,c,3}}{RT_{t,c,3}} = \frac{\gamma}{\gamma-1} \frac{p_{t,c,3}}{H_{t,c,3}} \left(\frac{H_{c,3}}{H_{t,c,3}}\right)^{\frac{1}{\gamma-1}} \tag{20}$$

where R is the gas constant.

Computations at Exit

5. The first step in computing the flow conditions and gas state at the exit is to find the conditions at the blade roots. Because the Mach number increases with decreasing r_3, and because the efficiency of normal shock compression drops rapidly for Mach numbers increasing above 1.4, a limit of $M_{h,3} = 1.4$ is taken at the root. There are two possible procedures for the next step.

(a) The maximum flow at the blade roots is assumed by setting $M'_{h,3} = 1.0$. With these values for the relative and absolute Mach numbers, equation (17) then determines $V_{u,h,3}$,

and $H_{h,3}$ is then computed from equation (16). Equation (15) is then employed to find $V_{h,3}$ and $H_{t,h,3}$; $V_{a,h,3}$ is computed by a right triangle formula. In completing a design begun on such a basis, it was found that the flow limitation occurred at the entrance rather than the exit and the condition $M'_{h,3} = 1.0$ was therefore discarded.

(b) An alternative procedure assigns several values of $H_{t,h,3}$ for each $r_{h,3}$. When the entrance flow is computed for each case, it is found that this flow could be accommodated at some radius for the root at the exit. Of the values of the exit root radius thus found, that which is equal to the assumed $r_{h,3}$ then gives the desired $H_{t,h,3}$. For any assumed value of $H_{t,h,3}$, the procedure would consist of first finding $H_{h,3}$ and $V_{h,3}$ from equation (15). Equation (14) is solved for $V_{u,h,3}$ and $V_{a,h,3}$ then found, thus determining all needed flow conditions at the blade roots.

6. In computing the variation in fluid state and flow conditions at the exit, $H_{t,3}$ is assumed to vary linearly with radius between the value at the case and that at the blade roots. Equation (13) gives H_3 and (12) determines $V_{u,3}$. Then

$$(V_3)^2 = 2(H_{t,3} - H_3)$$

$$(V_{a,3})^2 = (V_3)^2 - (V_{u,3})^2$$

and by assuming isentropic conditions at the exit

$$\rho_3 = \rho_{c,3} \left(\frac{H_3}{H_{c,3}} \right)^{\frac{1}{\gamma - 1}} \tag{21}$$

For correlation of the entrance and exit streamlines, the mass flow W_3 between the case and a cylinder of radius r_3 is required.

$$W = 2\pi \int_{r_3}^{r_{c,3}} \rho_3 V_{a,3} r_3 \, dr_3 \tag{22}$$

Computations at Entrance

7. Computations of flow at the entrance use equation (18), which gives

$$r_1 V_{u,1} = \frac{1}{\omega} (H_{t,1} - H_{t,3}) + r_3 V_{u,3} \qquad (23)$$

The entering moment of momentum $r_1 V_{u,1}$ is therefore known as a function of r_3, the radius at which that element of gas leaves the impeller. However, the value of the mass flow W_1 between radius r_1 and $r_{c,1}$ is the same as that between r_3 and $r_{c,3}$ for the same streamline; that is,

$$W(r_1) = -2\pi \int_{r_{c,1}}^{r_1} \rho_1 V_{a,1} r_1 \, dr_1$$

$$W(r_1) = -2\pi \int_{r_{c,3}}^{r_3} \rho_3 V_{a,3} r_3 \, dr_3 = W(r_3) \qquad (24)$$

establishes a relation between the corresponding r_1 and r_3 for any streamline. (The mass flow density $\rho_1 V_{a,1}$ is not yet known.) At the exit $r_3 V_{u,3}$ is a known function of W and equation (23) therefore also gives $r_1 V_{u,1}$ as a function of W. Equation (5) gives

$$\frac{d(V_{a,1})^2}{dW} = -\frac{1}{(r_1)^2} \frac{d(r_1 V_{u,1})^2}{dW} \qquad (25)$$

which cannot be solved directly for $(V_{a,1})^2$ as a function of W because r_1 is not known as a function of W. The quantity $\frac{d(r_1 V_{u,1})^2}{dW}$ is a known function of W, however, and can be evaluated

$$\frac{d(r_1V_{u,1})^2}{dW} = 2(r_1V_{u,1})\frac{dr_3}{dW}\frac{d}{dr_3}\left(r_3V_{u,3} - \frac{H_{t,3}}{\omega}\right)$$

But

$$\frac{dr_3}{dW} = -\frac{1}{2\pi r_3 \rho_3 V_{a,3}}$$

Also, $H_{t,3}$ and $(V_{u,3})^2/r_3$ are linear functions of r_3; consequently

$$\frac{dH_{t,3}}{dr_3} = \frac{H_{t,3c} - H_{t,3h}}{r_{c,3} - r_{h,3}}$$

and

$$\frac{d}{dr_3}(r_3V_{u,3}) = \frac{3V_{u,3}}{2} + \frac{(r_3)^2}{2V_{u,3}}\frac{\left[(V_{u,c,3})^2/r_{c,3}\right] - \left[(V_{u,h,3})^2/r_{h,3}\right]}{r_{c,3} - r_{h,3}}$$

Therefore

$$\mu \equiv -\frac{d(r_1V_{u,1})^2}{dW} = \frac{r_1V_{u,1}}{\pi r_3 \rho_3 V_{a,3}}$$

$$\times\left\{\frac{3V_{u,3}}{2} + \frac{r_3^2}{2V_{u,3}(r_{c,3} - r_{h,3})}\left[\frac{(V_{u,c,3})^2}{r_{c,3}} - \frac{(V_{u,h,3})^2}{r_{h,3}}\right] - \frac{H_{t,c,3} - H_{t,h,3}}{(r_{c,3} - r_{h,3})}\right\} \quad (26)$$

can be evaluated from exit computations as a function of W before solving for the entrance flow. Now equation (25) can be written

$$\frac{d(V_{a,1})^2}{dW} = \frac{\mu}{(r_1)^2} \quad (27)$$

and equation (24) can be expressed

$$\frac{d(r_1)^2}{dW} = -\frac{1}{\pi\rho_1 V_{a,1}} \tag{28}$$

The system of equations (27) and (28) can be numerically integrated by the Kutta-Runge method.

Another scheme of good accuracy for this special system was devised. Equation (27) can be expressed

$$\frac{d(V_{a,1})^2}{d(r_1 V_{u,1})^2} = -\frac{1}{(r_1)^2}$$

or

$$\frac{dy}{dx} = -\frac{1}{(r_1)^2}$$

where for convenience $y = (V_{a,1})^2$, $x = (r_1 V_{u,1})^2$. Then

$$\frac{d^2y}{dx^2} = \frac{1}{(r_1)^4}\frac{d(r_1)^2}{dx} = \frac{1}{(r_1)^4}\frac{dW}{d(r_1 V_{u,1})^2}\frac{d(r_1)^2}{dW}$$

$$\frac{d^2y}{dx^2} = \frac{1}{\pi\rho_1 V_{a,1}\mu(r_1)^4} \tag{29}$$

A Taylor's series expansion for y is

$$y(x+\Delta) = y(x) + \Delta y'(x) + \frac{\Delta^2}{2}y''(x) + \frac{\Delta^3}{3!}y'''(x) +$$

or

$$y(x-\Delta) = y(x) - \Delta y'(x) + \frac{\Delta^2}{2}y''(x) - \frac{\Delta^3}{3!}y'''(x) + +$$

Then

$$y(x+\Delta) = 2y(x) - y(x-\Delta) + \Delta^2 y''(x) + + \tag{30}$$

and

$$y(x+\Delta) = y(x-\Delta) + 2\Delta y'(x) + \frac{1}{3}\Delta^3 y'''(x) + \tag{31}$$

In starting the solution, a small increment in $(r_1 V_{u,1})^2$ is used and the term $\frac{1}{3}\Delta^3 y'''(x)$ in equation (31) is neglected to obtain

$$(V_{a,1}{}^2)_b - (V_{a,1}{}^2)_a = -\left[\frac{2}{(r_1{}^2)_a + (r_1{}^2)_b}\right]\left[(V_{u,1}{}^2 r_1{}^2)_a - (V_{u,1}{}^2 r_1{}^2)_b\right] \tag{32}$$

as the difference in axial velocities squared at two inlet radial stations a and b for the estimated value of $(r_1{}^2)_b$. The mean value of $\rho_1 V_{a,1}$ for the step is then estimated, utilizing the guess for $(r_1{}^2)_b$ to compute the value of ρ_1 at the average position by means of the stagnation density and the velocity. With this mean value of $\rho_1 V_{a,1}$ for the step from a to b, a better estimate of $(r_1{}^2)_b$ is obtained from

$$(r_1{}^2)_b - (r_1{}^2)_a = -\frac{1}{\pi \rho_1 V_{a,1}}(W_b - W_a) \tag{33}$$

where W_b and W_a are known in advance for the corresponding step in $(r_1 V_{u,1})_b - (r_1 V_{u,1})_a$. The new value of $(r_1{}^2)_b$ can then be used again in equation (32) and the process repeated to find the value of $(r_1{}^2)_b$ that checks. After one small step has been taken, equation (30) is used because it neglects only the fourth and higher derivatives. The size of the interval can be doubled after the second step because of the higher accuracy of the formula. In the case of equation (30), the steps are uniform in $(r_1 V_{u,1})^2$. Then equations (30) and (29) give

$$(V_{a,1}{}^2)_d = 2(V_{a,1}{}^2)_b - (V_{a,1}{}^2)_a + \frac{1}{\pi(\rho_1 V_{a,1} \mu r_1{}^4)_b} \times \left[(r_1{}^2 V_{u,1}{}^2)_d - (r_1{}^2 V_{u,1}{}^2)_b\right]^2 \tag{34}$$

and parabolic (second degree) integration of (28) gives

$$(r_1^2)_d - (r_1^2)_b = -\left[\frac{(r_1^2 V_{u,1}^2)_d - (r_1^2 V_{u,1})_b}{12\pi}\right] \times \left[-\frac{1}{(\mu\rho_1 V_{a,1})_a} + \frac{8}{(\mu\rho_1 V_{a,1})_b} + \frac{5}{(\mu\rho_1 V_{a,1})_d}\right] \tag{35}$$

In equation (35), $(V_{a,1})_d$ and μ_d are known, but $(\rho_1)_d$ is not. If an estimate is made, then $(r_1^2)_d$ and hence

$$(V_{u,1}) = \frac{1}{r_1}(V_{u,1} r_1)$$

and finally ρ_1 can be computed. Equation (35) is repeatedly used until the estimated and computed values of $(r_1^2)_d$ agree. The method fails if $(r_1 V_{u,1})$ as a function of W is constant; in that case however, a much simpler method of solution is available because equation (25) indicates $(V_{a,1})^2$ is constant, and $(V_{u,1})^2$ and hence ρ are known functions of r_1. The solution of equation (28) by Simpson's rule then identifies the variation of r_1 with variations in W.

8. At this stage of the computations the entire velocity distribution at the entrance and the exit is known, and the mass flow is also known as a function of radial position at the entrance and the exit. Examination of the velocity diagrams indicates in some cases a radius at which it is desirable to set the blade root. Computation of the blade stress at the roots also imposes limitations. If the blades are tapered with increasing thickness toward the root, blocking of the flow area may indicate a desirable radius for the root. By such considerations, a blade-root radius is decided upon and a mass flow established for the assumed values of $r_{c,1}$ and $r_{h,3}$.

DESIGN OF IMPELLER

After the best gas velocity distribution has been computed at the entrance and exit, the next problem is to design an impeller between these planes to accomplish the desired turning of air.

Inducer Section

The inducer section is regarded as that portion of the impeller where the air receives an initial compression with no radial flow at the case. At the end of the inducer section, the flow area is made as large as possible by designing for no radial flow at the root. Conditions at the inducer exit are estimated by the differential equations of motion on the assumption of a certain prescribed relative velocity at the case. (See equation (18).) Inside the impeller

$$H_t = H + \frac{V^2}{2} = H_{t,1} + \omega(r_2 V_{u,2} - r_1 V_{u,1})$$

The quantity

$$H + \frac{1}{2} v^2 - \omega r V_u = H + \frac{1}{2} v^2 - \frac{1}{2} \omega^2 r^2 = H_{t,1} - \omega r_1 V_{u,1} \qquad (36)$$

is therefore constant for any one streamline, and the relative stagnation enthalpy $H + (v^2/2)$ changes on any streamline only as a result of change in the potential energy level $(u^2/2)$. Equation (4) is then

$$\frac{dH}{dr} = \frac{(V_u)^2}{r} = -\omega \frac{d}{dr_1}(r_1 V_{u,1}) \frac{dr_1}{dr} + \omega \frac{d}{dr}(r V_u) - \frac{1}{2} \frac{dV^2}{dr} \qquad (37)$$

In terms of relative velocity

$$\frac{d}{dr}\left(\frac{v^2}{2}\right) = -\frac{(v_u)^2}{r} - 2\omega v_u - \omega \frac{d}{dW}(r_1 V_{u,1}) \frac{dW}{dr} \qquad (38)$$

Continuity gives

$$\frac{dW}{dr} = -2\pi r \rho v_a$$

In accounting for the area blocked by the blades, the quantity $2\pi r - (Bd/\cos \psi)$ must be used for $2\pi r$ where

B number of blades

d blade thickness

ψ angle between direction of axis of rotation and intersection of blade surface with circular cylinder about axis of rotation

The corrected mass-flow equation is

$$\frac{dW}{dr} = -\left(2\pi r - \frac{Bd}{\cos \psi}\right) \rho v \cos \psi \tag{39}$$

For structural strength it is prescribed that radial lines through the blade tips be blade elements and consequently

$$\tan \psi = (r/r_c) \tan \psi_c \tag{40}$$

Isentropic conditions are assumed at any axial depth; from this assumption the density variation is estimated by means of

$$\rho = \rho_c \left(\frac{H}{H_c}\right)^{\frac{1}{\gamma-1}} \tag{41}$$

in conjunction with (36) rewritten

$$H = H_{t,1} - \omega r_1 V_{u,1} - \frac{1}{2} v^2 + \frac{\omega^2 r^2}{2} \tag{42}$$

The equation of motion is then

$$\frac{d(v^2/2)}{dW} = \left[\frac{1}{(2\pi r - Bd \sec \psi) \rho v \cos \psi}\right] \times \left[\frac{v^2}{r} \sin^2 \psi + 2v \omega \sin \psi\right] - \omega \frac{d(r_1 V_{u,1})}{dW} \tag{43}$$

This equation may be solved simultaneously with equation (39) by a step-by-step process such as the Kutta-Runge method. The quantity $\omega \frac{d}{dW}(r_1 V_{u,1})$ is a known function of W and is computed before the inducer section is designed. The boundary value for $v_2 = v_{c,2}$ is also known, but ψ_c is not. A solution is therefore obtained for several values of ψ_c and the one giving the desired value for r_h is selected.

The blades must be turned from the entrance direction rapidly, especially in the beginning because the blade thickness may cause a velocity rise before the diffusion process is begun. The velocity distribution at the blade tips is estimated on an assumed camber line by the stream-filament method as outlined in reference 1. A check for boundary-layer separation is then made from the calculated velocity distribution and the suitability of the assumed design so evaluated. Modifications in shape are indicated by the desired change in velocity. The rest of the inducer blade surface is shaped according to equation (40).

Mixed-Flow Section

From the end of the inducer section to the impeller exit, a smooth surface of revolution is assumed for the shape of the case, and on this surface the curve representing the blade shape at the tips is assumed. The blade surface is then obtained from equation (40). The quantities r_c and ψ_c are then known functions of the axial depth, and therefore ψ is known at every point. The boundary condition of constant v_c is attained by properly shaping the root. The equations utilized in this step are derived in appendix A, and are listed here for continuity. The mass flow between two surfaces that are meridional projections of the streamlines is

$$-dW = \rho v \left(2\pi r - \frac{Bd}{\cos \alpha}\right) \cos \alpha \, dn \tag{44}$$

and the variation in relative velocity is determined by

$$\frac{d(v^2/2)}{dW} = -\frac{v}{\rho\left(2\pi r - \frac{Bd}{\cos \alpha}\right)} \times \left[\frac{\cos \alpha}{R_m} - \left(\frac{2\omega}{v} + \frac{\sin \alpha}{r}\right) \frac{\sin \alpha \cos \varphi}{\cos \alpha}\right] - \frac{d(\omega r_1 V_{u,1})}{dW} \tag{45}$$

where

α angle between velocity and meridional component

dn element of length in meridional plane normal to meridional velocity component

R_m radius of curvature of meridional projection of streamline

φ angle between meridional component and axis of rotation

If the blade consists of radial elements then

$$\tan \psi = \frac{r}{r_c} \tan \psi_c = \frac{\tan \alpha}{\cos \varphi} \tag{46}$$

Fluid density is related to that at the case and the enthalpy of the fluid by

$$\frac{\rho}{\rho_c} = \left(\frac{H}{H_c}\right)^{\frac{1}{\gamma-1}} \tag{47}$$

The density at the case ρ_c is computed on the assumption of constant efficiency during the compression process. Equation (46) is evaluated on a plane normal to the axis, and equation (47) is evaluated along the curve n, which consists of the line elements dn. An infinite number of blades and constant entropy along the n-curves are assumed. This system of equations is solved by taking small increments in the mass flow and evaluating the position of the streamline next to and inward from the one already known. The velocity is also evaluated at this streamline. The new streamline position is computed throughout the whole impeller before moving on to the next streamline. By this method it is possible to evaluate R_m and solve the equation. When the entire mass flow is thus accounted for, the shape of the hub is outlined by the last streamline.

Impeller Design Dimensions and Performance

The foregoing system of computations resulted in an impeller with the following design dimensions and performance characteristics:

Dimensions:

Radius of case at entrance, inches	5.62
Radius of case at exit, inches	7.00
Radial blade clearance, inch	.040
Radius of root at entrance, inches	2.75
Radius of root at exit, inches	5.90

Flow Characteristics at Exit:

Absolute Mach number at case	1.28
Absolute Mach number at root	1.40
Relative Mach number at case	.60
Relative Mach number at root	.75
Rotation velocity component, feet per second	1400
Axial velocity component at case, feet per second	710
Axial velocity component at root, feet per second	840
Impeller velocity at 7-inch radius, feet per second	1480

Performance:

Average pressure ratio	3.5
Mass flow, pounds per second	19.7
Efficiency near case	.85

The conditions at the exit are shown in figure 2 and those at the entrance in figure 3. Because of the constant entropy assumed at the exit the efficiency of compression is lower for streamlines near the root because of the lower work input.

EVALUATION OF DESIGN PROCEDURE

The fundamental objective of the design method was to find sufficient reasonable restricting conditions on the types of flow so that the number of variable design parameters would be as small as possible. The highest air-flow capacity design for variation of these parameters could then be found with a reasonable amount of labor. Some of these restrictions are quite arbitrary, such as the energy conversion possible in the inducer and the limitation of the absolute Mach number to 1.4 which was chosen because of the high efficiency of normal shock compression at this value. However, efficient diffusers can be designed at higher Mach numbers by utilizing oblique shocks.

More exact calculations of flow detail are also desirable, especially at the impeller entrance where radial flows exist.

More detail of the velocity distribution on the blade surfaces inside the impeller is required to account for three-dimensional flows. To utilize such a knowledge to the utmost, however, solution of the equations for the boundary-layer flow on the rotating blades is required in order to decide what is a good velocity distribution. No such solution exists.

One can therefore say that the design procedure is partly rational and partly empirical. Because the analytical solution of these flow problems is not in immediate prospect, experimental techniques must provide some of the information required for the step-by-step improvement of this promising type of compressor.

Flight Propulsion Research Laboratory,
National Advisory Committee for Aeronautics,
Cleveland, Ohio.

APPENDIX A

EQUATIONS OF INTERNAL RELATIVE FLOW IN IMPELLER

The gas inside the impeller is assumed to flow on surfaces of revolution, which permits an extensive simplification of the equations of motion. For a compressible fluid with absolute velocity $\bar{V}$ and steady velocity $\bar{v}$ relative to the impeller, which rotates with angular velocity ω, the equation of motion is

$$\nabla \frac{v^2}{2} - \bar{v} \times (\nabla \times \bar{v}) + \frac{\nabla p}{\rho} = \omega^2 \bar{r} + 2\bar{v} \times \bar{\omega} + \bar{F}/\rho \qquad (1)$$

The bar over the symbol indicates a vector quantity; $\bar{F}$ is the force per unit volume exerted by viscous forces and bodies distributed in the fluid. The term

$$\omega^2 \bar{r} = \bar{u} \times \bar{\omega} = \omega^2 \nabla \frac{r^2}{2} = \nabla \frac{u^2}{2}$$

is the centrifugal force where

$\bar{u} = \bar{\omega} \times \bar{r}$ linear velocity of rotation

$\bar{V} = \bar{u} + \bar{v}$ absolute velocity

$2\bar{v} \times \bar{\omega}$ Coriolis force

From the laws of thermodynamics, the equation will be modified by expressing the pressure and density in terms of other gas-state functions

$$\frac{1}{\rho} \nabla p = \nabla H - T \nabla S = \nabla \left(H_t - \frac{V^2}{2} \right) - T \nabla S$$

In the section on inducer design, it was found that the quantity

$$h \equiv H_t - V_u \omega r = H_t - \bar{u} \cdot \bar{V} = H + \frac{v^2}{2} - \frac{u^2}{2} \qquad (2)$$

was constant on streamlines in the inducer. This quantity is introduced into the equations of motion in order to determine the conditions for which it is constant for streamlines in the impeller.

$$(1/\rho)\,\nabla p = \nabla h - T\nabla S + (\nabla u^2/2) - \nabla v^2/2$$

Equation (1) then becomes

$$\nabla h = T\nabla S + \bar{v} \times (2\bar{\omega} + \nabla \times \bar{v}) + \bar{F}/\rho \tag{3}$$

This equation shows that the condition for h constant on a streamline $(\bar{v}\cdot\nabla h = 0)$ is

$$T\,\frac{\partial S}{\partial s} = -F_v/\rho \tag{4}$$

where $\partial/\partial s$ is the derivative along a streamline and F_v is the component of $\bar{F}$ parallel to $\bar{v}$. The entropy rise is a result of friction, and hence F_v is a frictional component of force. The rest of the force is normal to the velocity vector $\bar{v}$ and is designated as a lift force $\bar{F}_l$. Because h is constant along any streamline, then changes in h may be determined from values on different streamlines at the impeller entrance. At the entrance h is constant for different streamlines at the same radius. Because the flow is assumed to be on surfaces of revolution, h is therefore constant on surfaces of revolution; that is,

$$\bar{u}\cdot\nabla h = 0$$

The only remaining component of ∇h is therefore normal to $\bar{v}$ and $\bar{u}$ and is parallel to the unit vector

$$\hat{n} = \frac{\bar{v} \times \bar{u}}{\sqrt{(\bar{v} \times \bar{u})^2}} \tag{5}$$

which is in the meridional plane and normal to the projection of $\bar{v}$ on that plane. If the assumption is made that ∇S is parallel to $\bar{v}$,

$$T\nabla S = -(\hat{t}F_v)/\rho$$

and

$$\bar{F}_l/\rho + \bar{v} \times (2\bar{\omega} + \nabla \times \bar{v}) = \hat{n}\,\frac{\partial h}{\partial n} = \nabla h$$

where $\hat{t}$ is a unit vector parallel to $\bar{v}$.

It is now assumed that the lift force $\overline{F}_l$ is on the surface of revolution formed by the stream sheet as well as normal to the velocity. Thus, $\overline{F}_l$ is normal to $\hat{n}$, and therefore,

$$\frac{\partial h}{\partial n} = \hat{n} \cdot \overline{v} \times (2\overline{\omega} + \nabla \times \overline{v}) \tag{6}$$

Equation (6) provides the basis for computation of the streamlines in the impeller.

For greater convenience the velocity is broken down into two components v_m the meridional component and v_u the rotational component. Then

$$\hat{n} \cdot \overline{v} \times \overline{\omega} = \overline{v} \cdot \overline{\omega} \times \hat{n} = \overline{v} \cdot \overline{u} \cos \varphi / r = v_u u \cos \varphi / r = v_u \omega \cos \varphi$$

Also,

$$\overline{v} \times \nabla \times \overline{v} = \nabla v^2/2 - \overline{v} \cdot \nabla \overline{v}$$

and

$$\overline{v} \cdot \nabla \overline{v} = (\overline{v}_m + \overline{v}_u) \cdot \nabla (v_m \hat{m} + v_u \hat{u})$$

$$= v_m{}^2 \frac{\partial \hat{m}}{\partial m} + \hat{m} v_m \frac{\partial v_m}{\partial m} + \quad + \text{etc.}$$

$$= \hat{n} \frac{v_m{}^2}{R_m} + \overline{v}_m \frac{\partial v_m}{\partial m} + \hat{u} v_m \frac{\partial v_u}{\partial m} + \hat{m} \frac{v_u}{r} \frac{\partial v_m}{\partial \theta}$$

$$+ \frac{v_m}{r} \overline{v}_u \sin \varphi - \frac{\hat{r}}{r} v_u{}^2 + \frac{\hat{u}}{r} v_u \frac{\partial v_u}{\partial \theta}$$

where $\frac{1}{r} \frac{\partial v_m}{\partial \theta}$ is the derivative in the direction of $\overline{u}$. Equation (6) becomes

$$\frac{\partial}{\partial n} \left[h - (v^2/2) \right] = 2 v_u \omega \cos \varphi - \frac{v_m{}^2}{R_m} + \frac{v_u{}^2}{r} \cos \varphi \tag{7}$$

Because the stagnation enthalpy is assumed to be uniform at the entrance to the impeller, equation (2) gives

$$\frac{\partial h}{\partial n} = - \frac{\partial(\bar{u}_1 \cdot \bar{v}_1)}{\partial n}$$

so that equation (7) becomes

$$\frac{\partial v}{\partial n} = - 2 \frac{v_u}{v} \omega \cos \varphi + \frac{v_m^2}{R_m v} - \frac{v_u^2}{vr} \cos \varphi - \frac{1}{v} \frac{\partial(\bar{u}_1 \cdot \bar{v}_1)}{\partial n}$$

If an infinite number of blades is assumed with loading and volume dispersed in the fluid, the variation of mass flow is

$$- dW = \rho v_m \left(2\pi r - \frac{Bd}{\cos \alpha} \right) dn \tag{8}$$

Then

$$\frac{\partial(v^2/2)}{\partial W} = - \left[\frac{v}{\rho \left(2\pi r - \frac{Bd}{\cos \alpha} \right)} \right]$$

$$\times \left[\frac{\cos \alpha}{R_m} - \left(\frac{2\omega}{v} + \frac{\sin \alpha}{r} \right) \frac{\sin \alpha \cos \varphi}{\cos \alpha} \right] - \frac{d}{dW} (\bar{u}_1 \cdot \bar{v}_1) \tag{9}$$

The quantity $d(\bar{u}_1 \cdot \bar{v}_1)/dW$ is a known function of the particular streamline in application of this equation to impeller design.

The angle ψ between the axial direction and the curve formed by the intersection of the blade with the circular cylinder about the axis is related to α and φ by

$$\tan \psi = \frac{\sin \alpha}{\cos \varphi \cos \alpha} = \frac{\tan \alpha}{\cos \varphi} \tag{10}$$

If the blades consist of radial elements,

$$\tan \psi = \frac{r}{r_c} \tan \psi_c$$

APPENDIX B

SYMBOLS

The following symbols are used in the text and the appendix:

a	sonic velocity
B	number of blades
d	thickness of blade
F	force exerted on fluid by blades and viscous forces
f	slip factor for discharge tangential velocity
H	enthalpy of gas
M	Mach number of absolute velocity
M'	Mach number of relative velocity
n	coordinate on curve in meridional plane and normal to the relative velocity
p	pressure
R	gas constant
R_m	radius of curvature of meridional projection of streamline
r	radial distance from axis of rotation
S	entropy of gas
s	coordinate along a streamline
T	absolute temperature
u	linear velocity of rotating impeller
V	absolute velocity of gas
v	relative velocity of gas
W	mass flow between two stream surfaces of revolution

α angle between meridional component and resultant relative gas velocity

γ ratio of specific heats of gas

μ $-\frac{d(r_1 V_{u,1})^2}{dW}$

ρ gas density

φ angle between meridional and axial components of gas velocity

ψ $\tan^{-1}(v_u/v_a)$

ω angular velocity of impeller

Unit vectors:

$\hat{t}$ in direction of relative velocity $\bar{v}$

$\hat{u}$ in direction of velocity of impeller $\bar{u}$

$\hat{n}$ in meridional plane normal to stream surface of revolution $\left(\hat{n} = \frac{\hat{u} \times \hat{t}}{\sqrt{(\hat{u} \times \hat{t})^2}}\right)$

$\hat{m}$ parallel to projection of relative velocity curve on meridional plane. (Normal to $\hat{n}$ and $\hat{u}$)

Subscripts:

1 impeller entrance

2 inducer exit

3 impeller discharge

a axial velocity component

c case value (at blade tips)

h hub value (at blade roots)

l lift

m meridional velocity component

r radial velocity component

t stagnation state

u rotational velocity component

REFERENCE

1. Stodola, A.: Steam and Gas Turbines. Vol. II. McGraw-Hill Book Co., Inc., 1927, pp. 992-994. (Reprinted, Peter Smith (New York), 1945.)

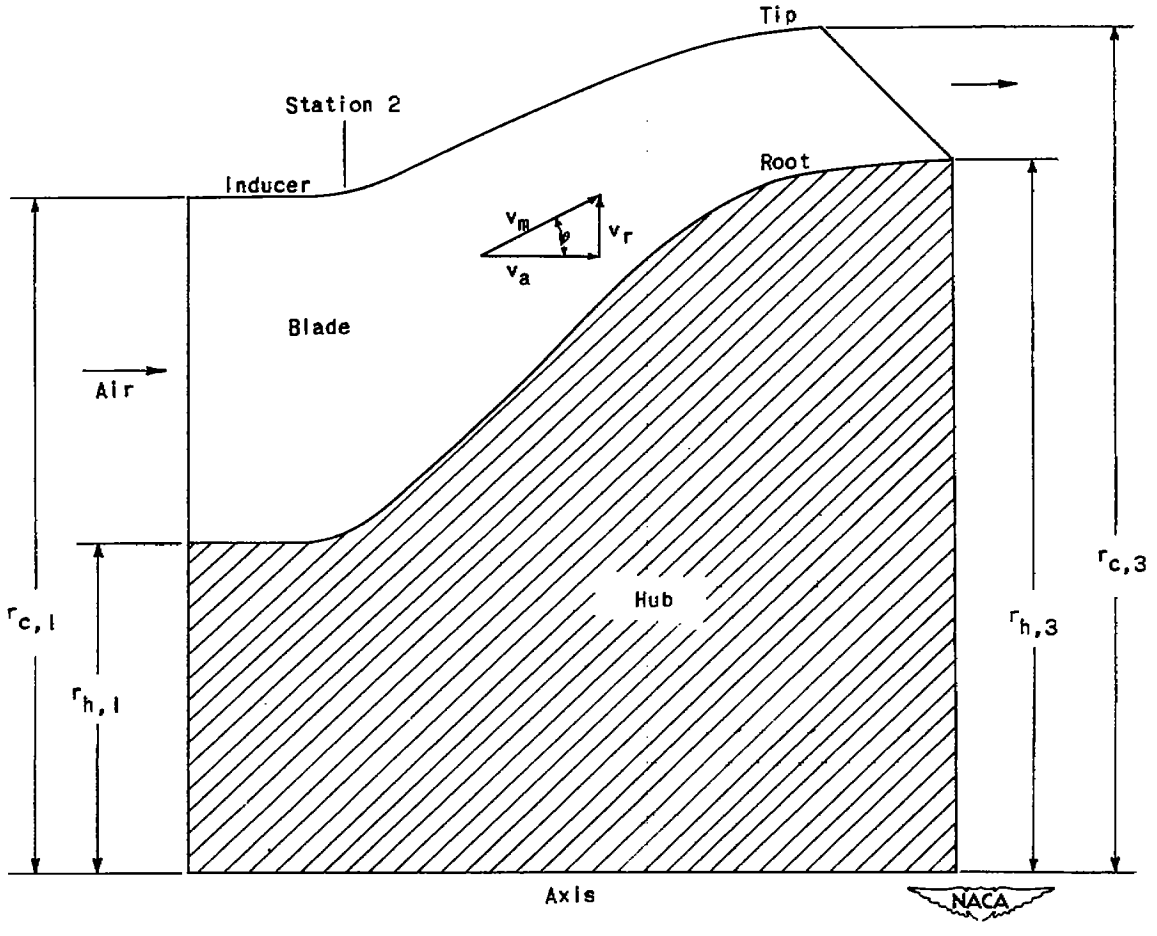

Figure 1.- Experimental axial-discharge mixed-flow impeller.

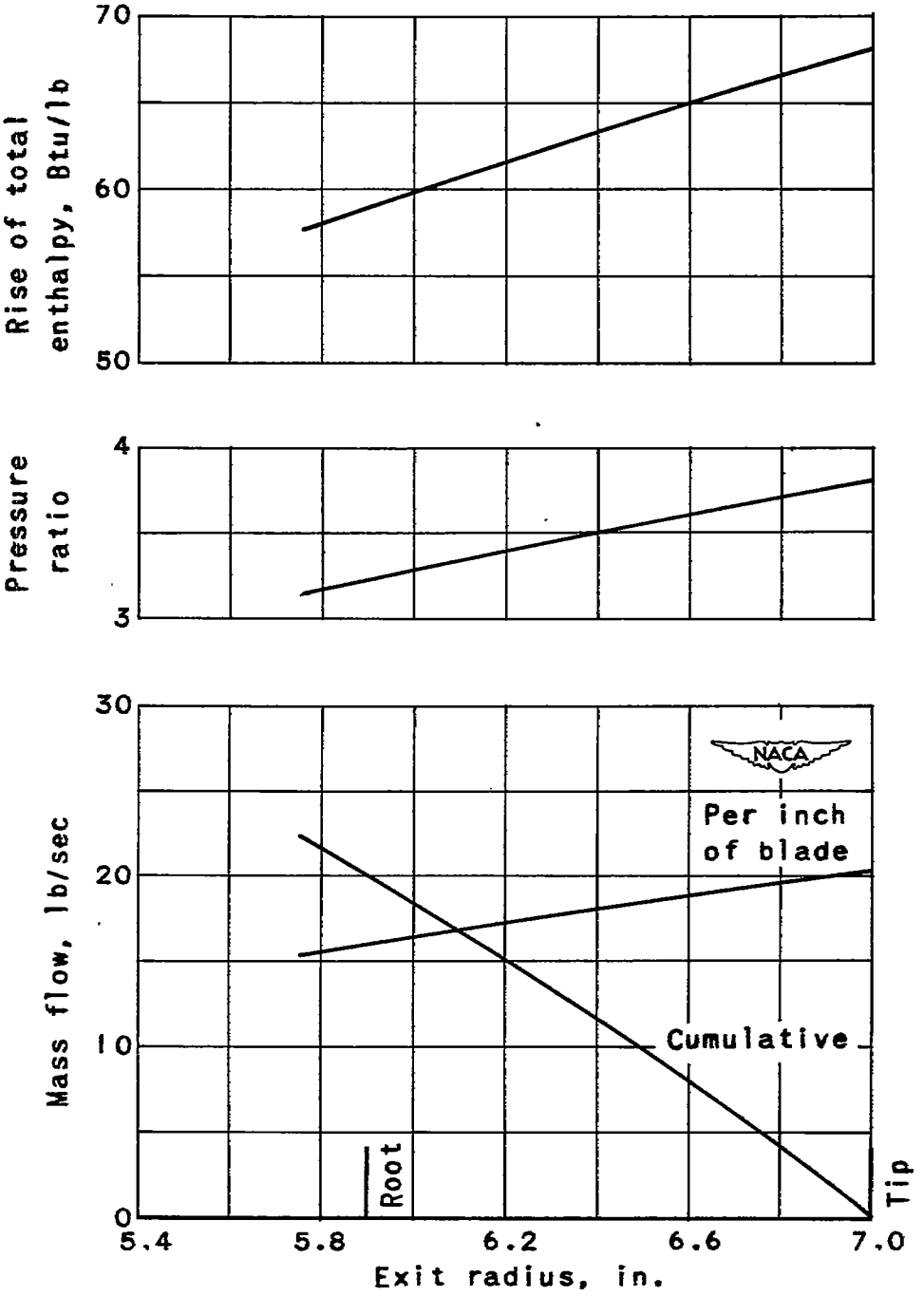

Figure 2. – Mass flow, pressure, and enthalpy at impeller exit.

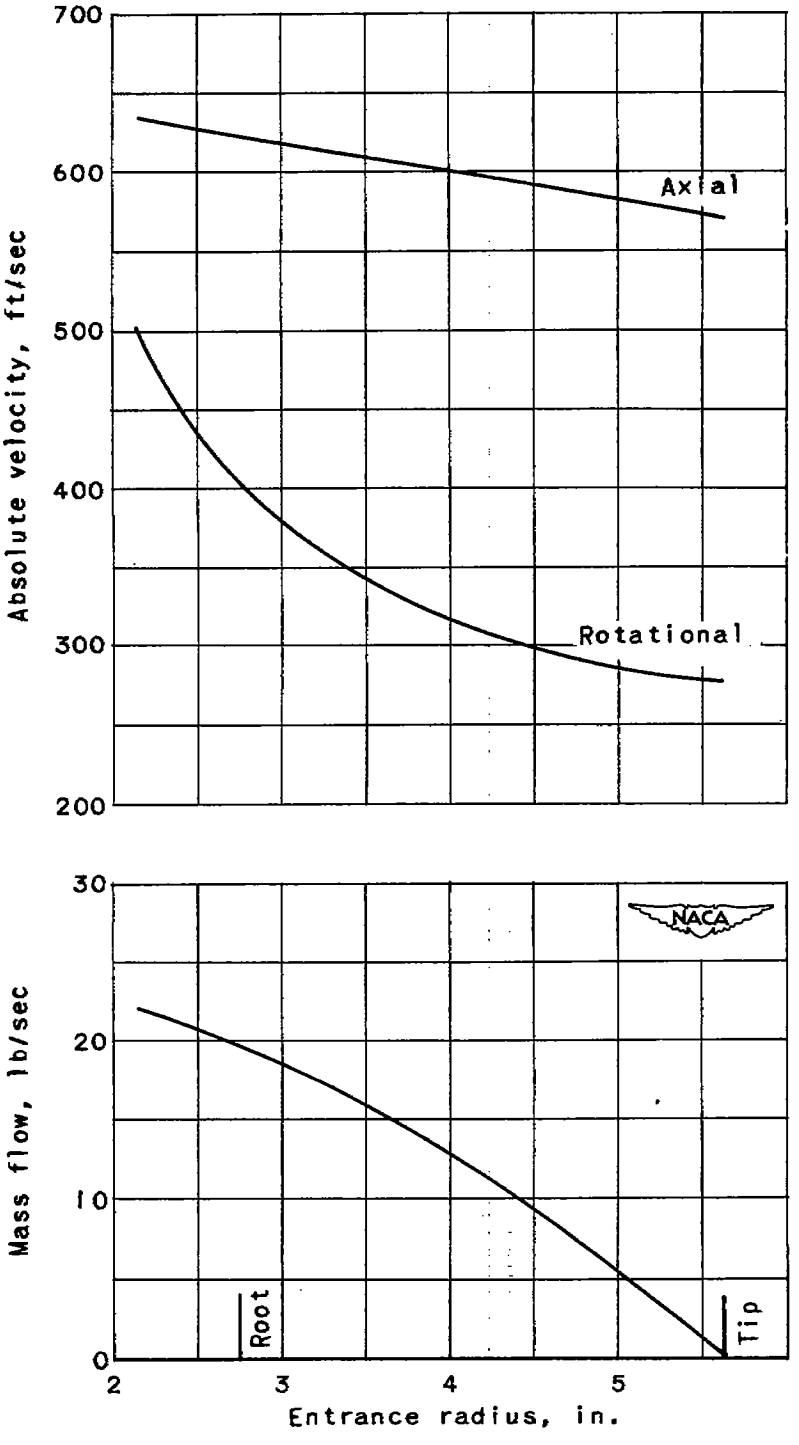

Figure 3. - Mass flow and absolute velocity at impeller entrance.